Journal of the Ceramic Society of Japan 123 [10] 942-948 2015 Paper

Structure and dissolution behavior of $MgO–P_2O_5–TiO_2/Nb_2O_5$ (Mg/P ≥ 1) invert glasses

Sungho LEE, Hirotaka MAEDA, Akiko OBATA, Kyosuke UEDA,*
Takayuki NARUSHIMA* and Toshihiro KASUGA†

Department of Frontier Materials, Graduate School of Engineering, Nagoya Institute of Technology, Gokiso-cho, Showa-ku, Nagoya 466–8555, Japan
***Department of Metallurgy, Materials Science and Materials Processing, Graduate School of Engineering, Tohoku University, 6–6–02 Aoba, Aramaki, Aoba-ku, Sendai 980–8579, Japan**

Magnesium phosphate glasses exhibit unusual properties and were classified as 'anomalous phosphate glasses', because magnesium is attributed to a variation of the oxygen coordination number from 6 to 4. Magnesium in phosphate glasses acts as an intermediate oxide and its role was determined, relating to the phosphate chain length. In the present work, $MgO–P_2O_5–TiO_2/Nb_2O_5$ glasses with Mg/P ratio between 1.00 and 1.36 were successfully prepared by a melt–quenching method. Magnesium in the glasses worked as a network former to form P–O–Mg bonds, which are cross-linked short phosphate chains that improved the glass-forming ability. Intermediate oxides (i.e., TiO_2 and Nb_2O_5) in the glasses also cross-linked short phosphate chains to form P–O–Ti/Nb bonds. The chemical durability of the glasses decreased with an increase in the Mg/P ratio, because magnesium, which entered the phosphate network, weakened the glass network to induce hydrolysis. The dissolution rate of Ti^{4+} and Nb^{5+} ions showed a decreasing tendency with an increase in the Mg/P ratio. The surfaces of the glasses were considered to be covered with gel-like oxide layers containing titanium or niobium and phosphate.

Key-words : Biomaterial, Phosphate glass, Invert glass, Magnesium, Niobium, Titanium, Structure

[Received June 29, 2015; Accepted July 17, 2015]

1. Introduction

Magnesium phosphate glasses exhibit unusual properties and were classified as 'anomalous phosphate glasses' by Kodrdes et al.[1)–3)] The anomalous properties of magnesium phosphate glasses are attributed to the variation of the Mg–O coordination number from 6 to 4.[1)] Many researchers have focused on $MgO–P_2O_5$ binary glasses and discussed their structures.[4)–13)] Magnesium in phosphate glasses acts as a network modifier and/or former depending on their composition, i.e., intermediate oxides: the role is determined by the phosphate chain length.[10),12)] Anomalous behavior of magnesium were introduced also in multi-component phosphate glasses to improve their properties.[14)–21)] MgO-containing phosphate invert glasses have also been the focus of research in our group, and the glasses showed improvement in their glass-forming ability and processing.[22),23)] Magnesium is one of the important elements in the human body; the Mg^{2+} ion concentration in the body has been reported to influence bone strength.[24)] In addition, Mg^{2+} ions have been reported to accelerate osteoblast adhesion and enhance cell proliferation and differentiation.[25)–28)]

Calcium phosphate invert glasses containing titanium or niobium have been the focus of research in our group.[29),30)] The glasses consist of short phosphate groups, such as ortho- and pyrophosphates (Q_p^0 and Q_p^1). P–O–Ti/Nb bonds in the glasses support the formation of the glass network.[29),31)] Titanium-containing calcium phosphate invert glasses indicated in vitro and in vivo bioactivity.[32),33)] Niobium-containing calcium phosphate glasses enhance the differentiation of osteoblast-like cells,[30)] and the crystallized glass shows apatite-forming ability in a simulated body fluid.[34)]

Amorphous calcium phosphate films were prepared on metallic titanium using a radiofrequency magnetron sputtering (RF-sputtering) method by Narushima et al.[35)] The thicknesses of the films were 0.5–1 μm, and the tensile bonding strengths between the film and titanium were measured to be over 60 MPa when the epoxy glue used in the test was detached without damaging the film.[36)]

Magnesium-containing phosphate invert glasses with titanium or niobium may be one of the candidates for amorphous film preparation using a RF-sputtering method. The film would be expected to enhance cell adhesion, proliferation, and differentiation. The glass structures and dissolution behaviors must be clarified for using the RF-sputtering method. In this work, we focused on phosphate invert glasses containing a large amount of MgO with TiO_2 or Nb_2O_5, and the invert glasses were prepared via a conventional melt-quenching method. The structures and dissolution behaviors of the glasses as well as their fundamental properties were examined to design new biomaterials.

2. Experimental procedures

Titanium- or niobium-containing magnesium phosphate invert glasses with nominal compositions of $x\mathrm{MgO}\cdot(90-x)\mathrm{P_2O_5}\cdot 10\mathrm{TiO_2}$ (mol%, $x = 60$–66, denoted by TiMg-IGs) and $y\mathrm{MgO}\cdot(94.5-y)\mathrm{P_2O_5}\cdot 5.5\mathrm{Nb_2O_5}$ (mol%, $y = 63$–69, denoted by NbMg-IGs) were prepared, as shown in **Table 1**. Glass batches were prepared using MgO (99.0%), H_3PO_4 (85% liquid), TiO_2 (99.5%), and Nb_2O_5 (99.9%). All reagents were obtained from Kishida Chemical Co., Japan. The glass compositions were

† Corresponding author: T. Kasuga; E-mail: kasuga.toshihiro@nitech.ac.jp

DOI http://dx.doi.org/10.2109/jcersj2.123.942

Table 1. Nominal and analyzed glass compositions and nominal Mg/P ratios of the glasses (glass code). The analyzed compositions are shown in round brackets with the standard deviation

Mg/P ratio (Glass code)	Composition/mol %				Composition/atom %			
	MgO	P_2O_5	TiO_2	Nb_2O_5	Mg	P	Ti	Nb
MgO–P_2O_5–TiO_2 Glasses (TiMg-IGs)								
1.00	60 (59.1 ± 0.6)	30 (32.7 ± 0.3)	10 (8.2 ± 0.3)	—	46	46	8	—
1.09	62 (58.4 ± 0.9)	28 (31.1 ± 0.7)	10 (10.5 ± 0.7)	—	48	44	8	—
1.24	64 (63.6 ± 1.8)	26 (29.1 ± 1.0)	10 (7.3 ± 0.8)	—	51	41	8	—
1.36	66 (67.2 ± 3.2)	24 (25.1 ± 1.6)	10 (7.7 ± 1.6)	—	53	39	8	—
MgO–P_2O_5–Nb_2O_5 Glasses (NbMg-IGs)								
1.00	63 (61.2 ± 1.1)	31.5 (33.1 ± 1.3)	—	5.5 (5.7 ± 0.2)	46	46	—	8
1.09	65 (60.9 ± 2.2)	29.5 (33.1 ± 2.3)	—	5.5 (6.0 ± 0.4)	48	44	—	8
1.24	67.5 (64.8 ± 0.6)	27 (29.8 ± 0.5)	—	5.5 (5.5 ± 0.2)	51	41	—	8
1.36	69 (69.2 ± 1.7)	25.5 (25.7 ± 1.6)	—	5.5 (5.3 ± 0.2)	53	39	—	8

adjusted by varying the atomic ratios of Mg, P, and Ti or Nb. The reagents were mixed with distilled water to make a slurry, and the mixture was dried under an infrared lamp overnight and then stored at 140°C. The batches were melted in a platinum crucible at 1500°C for 30 min and then quenched by pressing using two stainless-steel plates to prevent crystallization. The resulting glass compositions were examined by energy dispersive X-ray spectroscopy (EDX, JED-2300, JEOL Co., Japan), and the results are shown in Table 1.

The glass transition temperature (T_g) and crystallization temperature (T_c, defined as the onset of crystallization) of the glasses were obtained from differential thermal analysis (DTA; heating rate: 5 K/min, Thermo plus TG8120, Rigaku Co., Japan). The glassification degree was calculated as $(T_c - T_g)/T_g$ (K/K)[37] and used as an indicator of glass-forming ability.

Solid-state ^{31}P magic angle spinning nuclear magnetic resonance (MAS-NMR) spectra were measured to clarify the phosphate structures in the glasses at 242.955 MHz in a 3.2 mm rotor, spinning at 15 kHz (JNM-ECA600II, JEOL Co., Japan). A single pulse experiment with 0.1 μs pulse width, 5 s recycle delay and cumulated number of 256 was performed for each sample. The chemical shift was referenced to the signal of $NH_4H_2PO_4$ as 1.0 ppm.

The glass structure was investigated by laser Raman spectroscopy on quenched glass samples in the region of Raman shifts between 500 and 1300 cm^{-1} (NRS-3300, 532.08 nm, JASCO Co., Japan).

Glass samples were pulverized and sieved to particle sizes between 125 and 250 μm. Tris buffer solution (TBS) was prepared by dissolving 6.118 g of tris(hydroxymethyl)aminomethane [$NH_2C(CH_2OH)_3$, Kishida Chemical Co., Japan] in 1 L of distilled water at 37°C and adjusting to a pH value of 7.4 using 1 N hydrochloric acid. Fifteen mg of the glass powders were soaked in 15 mL of TBS at 37°C for 7 days (n = 3). The concentrations of Mg^{2+}, P^{5+}, Ti^{4+}, and Nb^{5+} ions in TBS after soaking the glass powders were measured by inductively coupled plasma atomic emission spectroscopy (ICP-AES, ICPS-7000, Shimadzu Co., Japan). Their dissolution rates were calculated using the following equation,

$$\text{Dissolution rate (\%)} = \frac{1000 \times (x/W_{\text{Atom}})}{([Atom_{\text{Rate}}] \times W_{\text{sample}})/(M_{\text{glass}} \times V_{\text{solution}})} \times 100 \quad (1)$$

where x (ppm) is the ion amount dissolved in the TBS after soaking, measured by ICP-AES. W_{Atom} is the atomic weight of the ion, and $[Atom_{\text{Rate}}]$ is the atomic rate of the ion calculated from the nominal glass composition. W_{sample} (g), M_{glass}, and V_{solution} (L) are the weight of the sample soaked, the molecular weight of the glass, and the volume of solution used for soaking (i.e., TBS), respectively.

3. Results

In compositions with Mg/P ratio <1.24 (in nominal composition), optically clear glasses were obtained, while in compositions with Mg/P ratio ≥1.24, partially crystallized glasses were obtained. For the following experiments, the crystalline (opaque) parts were removed manually. The analyzed compositions of the glasses are shown in Table 1. The amount of magnesium oxide and phosphate were varied by approximately 4 mol %. The amount of titanium oxide in the TiMg-IGs was varied by approximately 3 mol %. The amount of niobium oxide in the NbMg-IGs was showed reasonably close to the nominal composition. The analyzed compositions may show low accuracy, because magnesium is a light element, which leads to a low accuracy with EDX, and the phosphorus $K\alpha$ level (2.013 eV) overlaps the niobium $L\alpha$ level (2.166 eV). It was difficult to accurately determine the composition using EDX. The glass codes (Mg/P ratio) according to the nominal compositions are used in the following discussion.

Figure 1 shows the T_g, T_c, and glassification degree of the glasses. The T_g value increased with the Mg/P ratio; the T_g values increased from 639 to 665°C and from 646 to 663°C for TiMg-IGs and NbMg-IGs, respectively. The T_c values showed no significant difference irrespective of the Mg/P ratio; the values varied in the ranges of 705 to 717°C and 718 to 729°C for TiMg-

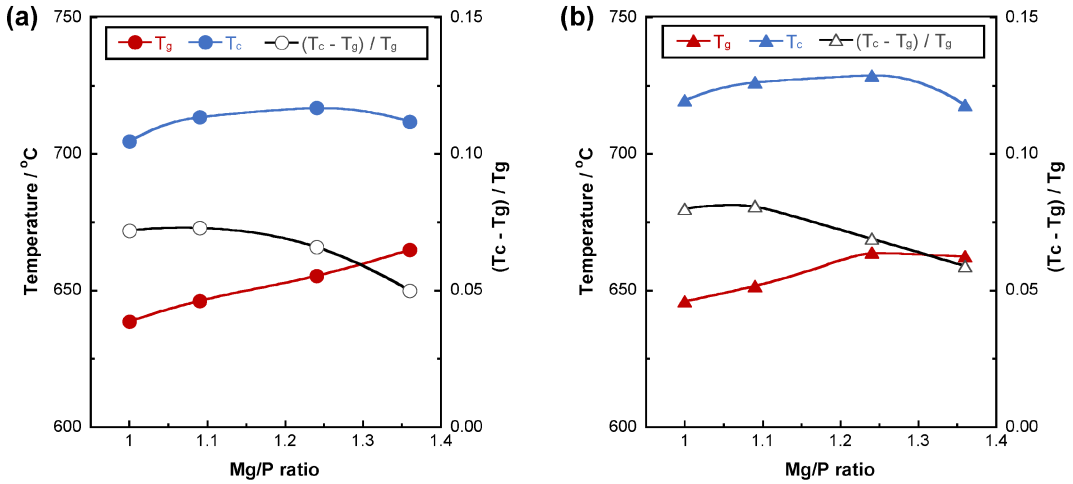

Fig. 1. Glass transition temperature (T_g), crystallization temperature (T_c), and glassification degree $[(T_c - T_g)/T_g]$ for (a) TiMg-IGs and (b) NbMg-IGs.

IGs and NbMg-IGs, respectively. The glassification degree decreased with increasing the Mg/P ratio; the values for TiMg-IGs decreased from 0.07 to 0.05, and those for NbMg-IGs decreased from 0.08 and 0.06.

^{31}P MAS-NMR spectra of the glasses are shown in **Figs. 2**(a) and 2(b). The center peaks between 10 and −30 ppm can be assigned to Q_p^0 and Q_p^1 units. The experimental spectra were simulated by assuming Gaussian lines for Q_p^0 and Q_p^1 units. In the spectra for TiMg-IGs and NbMg-IGs with Mg/P ratio of 1.36, a sharp peak was observed around 0 ppm, which originated from the crystalline magnesium phosphate, because it was not completely removed. The peak-integrated portions associated with the crystalline part were estimated to be 0.39 and 0.74% in TiMg-IG and NbMg-IG with Mg/P ratio = 1.36, respectively. Hereafter, trace amounts of the residual crystalline parts are believe to be able to excluded from the following discussion. The position of the fractured peak tops of Q_p^0 in TiMg-IGs and NbMg-IGs showed no significant difference irrespective of the Mg/P ratio. With an increase in the Mg/P ratio, the fractured peak top positions of Q_p^1 low-field shifted from −10.4 to −4.6 ppm and from −10.8 to −4.4 ppm for TiMg-IGs and NbMg-IGs, respectively, as shown in Figs. 2(c) and 2(d). The peak-integrated portions associated with Q_p^0 and Q_p^1 groups in the glasses increased and decreased linearly, respectively, with increasing the Mg/P ratio. Q_p^0 contents in TiMg-IGs and NbMg-IGs increased from 12 to 70% and from 13 to 67%, respectively, and Q_p^1 contents in TiMg-IGs and NbMg-IGs decreased from 88 to 30% and from 87 to 33%, respectively, with increasing the Mg/P ratio, as shown in Figs. 2(e) and 2(f).

The phosphate groups in the glasses showed Raman bands corresponding to Q_p^0 and Q_p^1 groups, as shown in **Figs. 3**(a) and 3(b), including the $(PO_4)_{sym}$ stretching mode of the non-bridging oxygen in Q_p^0 (980 cm^{-1}), the POP_{sym} stretching mode of the bridging oxygen in Q_p^1 (770 cm^{-1}), the $(PO_3)_{sym}$ stretching vibrations of the non-bridging oxygen in Q_p^1 (1060 cm^{-1}),[12] and the P–O stretch of Q_p^1 chain terminator (1160 cm^{-1}).[38] TiMg-IGs sample showed bands corresponding to the Ti–O stretching vibration of TiO_6 octahedron (660 cm^{-1}) and the Ti–O stretching vibration of TiO_4 tetrahedron (840 cm^{-1}).[39] NbMg-IGs sample showed bands corresponding to the Nb–O vibration of NbO_6 octahedron corner-linked in a three-dimensional network (655 cm^{-1}), the Nb–O vibration of NbO_4 tetrahedron (835 cm^{-1}), and the Nb–O bond vibration in isolated NbO_6 octahedral unit (915 cm^{-1}).[40),41] The experimental Raman spectra were simulated by assuming Gaussian lines, and the integrated peak intensities of the deconvoluted spectra were calculated. The integrated peak intensities of the spectra for the phosphate, Ti–O, and Nb–O groups were normalized by the sum of $I(POP_{sym}) + I[(PO_4)_{sym}] + I[(PO_3)_{sym}] + I$(P–O stretch Q_p^1 chain terminator), $I(TiO_6) + I(TiO_4)$, and $I(NbO_{6\_3D}) + I(NbO_4) + I(NbO_{6\_isolated})$, respectively [Figs. 3(c)–3(f)], where I denotes each peak amplitude. With an increase in the Mg/P ratio in TiMg-IGs and NbMg-IGs, the peak intensities associated with Q_p^0 group increased, and those associated with Q_p^1 group decreased [Figs. 2(c) and 2(d)]. With an increase in the Mg/P ratio in the glasses, the peak intensity associated with the tetrahedra (i.e., TiO_4 and NbO_4) increased, and those associated with the octahedra (i.e., TiO_6 and NbO_6) decreased [Figs. 3(e) and 3(f)].

Figure 4 shows ion-release percentages from the glasses into the TBS, relative to the original amount in the glasses. With an increase in the Mg/P ratio, the amount of Mg^{2+} and P^{5+} ions released from TiMg-IGs and NbMg-IGs increased from 25 to 48% and from 28 to 47%, respectively. The amount of Ti^{4+} ions released from TiMg-IGs decreased from 21 to 4%, and the amount of Nb^{5+} ions released from NbMg-IGs decreased from 23 to 11%. The insets in Figs. 4(c) and 4(f) are the surface SEM images of the glasses with Mg/P ratio = 1.36 after being soaked in the TBS for 7 days and their EDX spectra, respectively. The surface of TiMg-IGs and NbMg-IGs may be covered with a new layer composed of titanium or niobium and phosphate. EDX spectra also included a Mg peak, which would originate from the glasses under the newly formed layer.

4. Discussion

TiMg-IGs and NbMg-IGs showed an increase in T_g and a decrease in glassification degree with an increase in the Mg/P ratio. The glasses showed relatively high glassification degrees of 0.05 and 0.06 for TiMg-IG (Mg/P = 1.36) and NbMg-IG (Mg/P = 1.36), respectively. In our previous work, the glassification degree of $CaO–SrO–P_2O_5–Na_2O–TiO_2$ invert glasses [(Ca+Sr)/P ratio of 1.00] was between 0.02 and 0.05.[42] Therefore, TiMg-IGs and NbMg-IGs showed larger glassification degrees than $CaO–SrO–P_2O_5–Na_2O–TiO_2$ invert glasses. According to Dietzel's rule, MgO is an intermediate oxide.[43] Karakassides et al. reported that Mg^{2+} ion acts as a network former in phosphate glasses with a high MgO content, which consist of Q_p^0 and Q_p^1 groups.[12] In our

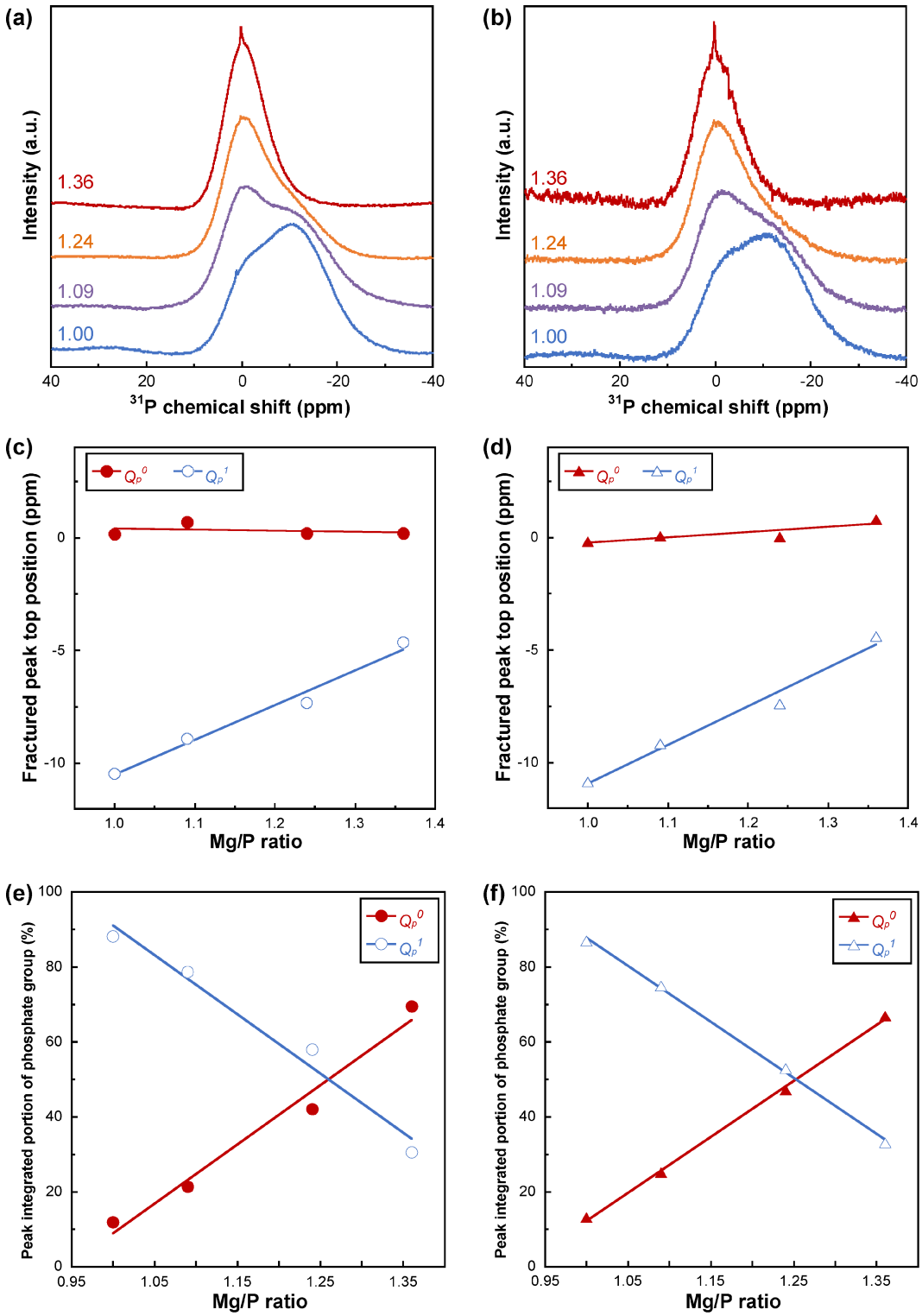

Fig. 2. ^{31}P MAS-NMR spectra for (a) TiMg-IGs and (b) NbMg-IGs, fractured peak top positions for (c) TiMg-IGs and (d) NbMg-IGs, and peak-integrated portions of phosphate groups for (e) TiMg-IGs and (f) NbMg-IGs as a function of the Mg/P ratio in the glass.

previous work, a magnesium phosphate invert glass also showed larger glass-forming ability than a calcium phosphate or strontium phosphate invert glass.[22] Magnesium ions in TiMg-IGs and NbMg-IGs act as a network former and may enter the phosphate network to apparently form P–O–Mg bonds, which cross-link short phosphate chains (Q_p^0 and Q_p^1)[23] to form longer structures. Thus, glasses can be obtained with Mg/P ratio $\leq$1.36 despite insufficient glass network formers (i.e., phosphate).

In Fig. 2, the fractured peak top position of Q_p^0 group showed no significant difference irrespective of composition. This means no significant change in the electron density of Q_p^0. With an increasing Q_p^0 in the glasses (i.e., increasing Mg/P ratio), Mg^{2+}

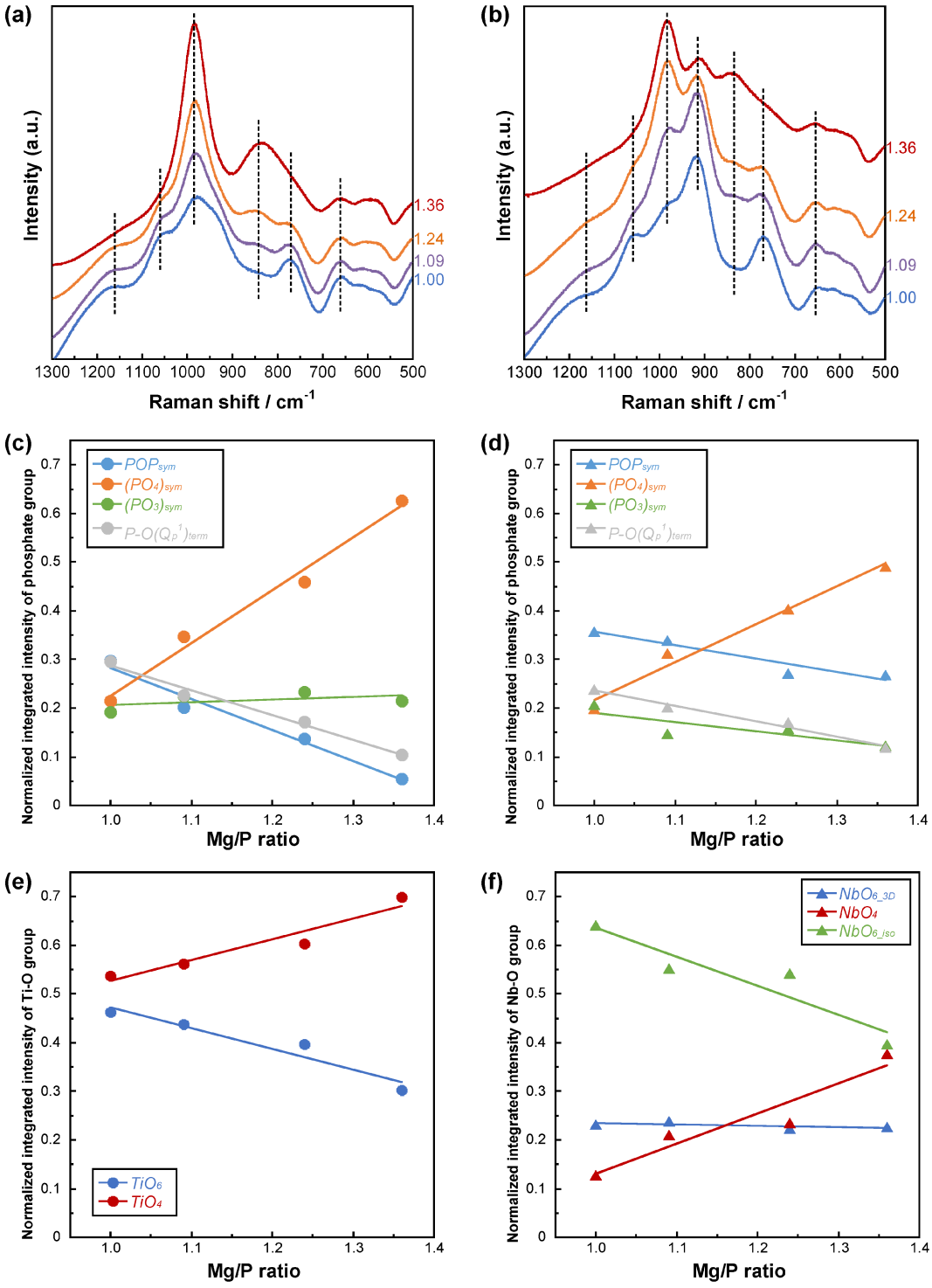

Fig. 3. Laser Raman spectra for (a) TiMg-IGs and (b) NbMg-IGs and normalized integrated peak intensities corresponding to phosphate groups of (c) TiMg-IGs and (d) NbMg-IGs, (e) Ti–O groups of TiMg-IGs, and (f) Nb–O groups of NbMg-IGs as a function of the Mg/P ratio in the glass.

ions preferentially bond with Q_p^0 groups, such as P–O–Mg; the fractured peak top position of Q_p^0 is unchanged. The fractured peak top position of Q_p^1 groups showed a low-field shift, which indicates a decrease in electron density with increasing the Mg/P ratio. Magnesium ions cross-link with Q_p^0 groups preferentially, and Q_p^1 groups have more chance to be influenced by titanium and niobium, which have larger field strengths compared to magnesium [Nb: 1.73, Ti: 1.04, Mg: 0.45 or 0.53 (4-fold or 6-fold coordination) valance/Å^2].[43] Therefore, electrons belonging to Q_p^1 groups would be pulled to the titanium or niobium side; the electron densities of Q_p^1 decrease with increasing the Mg/P ratio.

Our previous work reported that titanium-containing calcium phosphate invert glasses include P–O–Ti bonds, and their peak intensities in Raman spectra increased with increasing the TiO_2 content.[29] Titania in $TiO_2–P_2O_5$ glasses[44] and $TiO_2–ZnO–P_2O_5$ glasses[45] forms TiO_6 octahedral structure and links to phosphate

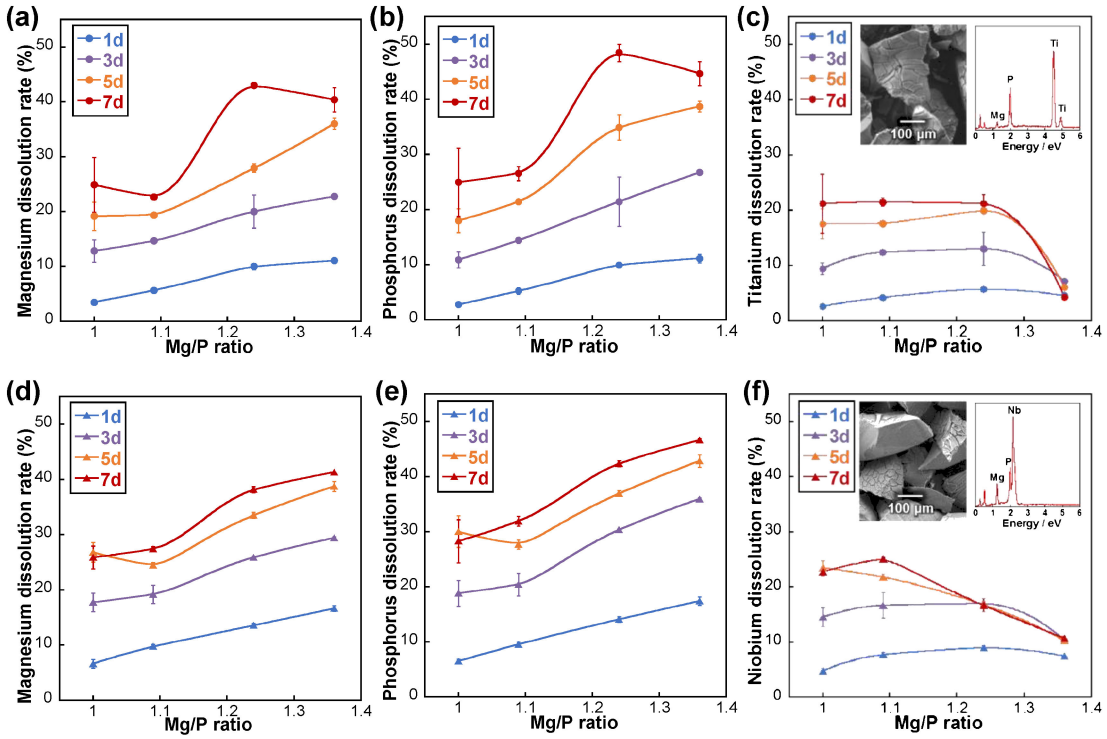

Fig. 4. Percentages of ions released into the TBS relative to the total amount in (a–c) TiMg-IGs and (d–f) NbMg-IGs for (a, d) Mg^{2+}, (b, e) P^{5+}, (c) Ti^{4+}, and (f) Nb^{5+} ions as a function of the Mg/P ratio in the glass. The insets in (c, f) show the surface SEM image of the glasses with Mg/P ratio of 1.36 after being soaked in TBS for 7 days and their EDX spectra.

groups, such as P–O–Ti bonds, when the glasses consist of Q_p^2 and Q_p^1. In P_2O_5–CaO–Na_2O–TiO_2 glasses consisting of Q_p^1, titania enters the glass network as TiO_4 tetrahedra connected to phosphate groups through the P–O–Ti bonds.[46] Niobate linking to P–O–Nb bonds takes NbO_6 octahedra when the glasses are composed of Q_p^2 and Q_p^1 groups.[31),47),48] Hsu et al. and Chu et al. reported that P–O–Nb bond forms, and the partial NbO_6 octahedron structure gradually turns into NbO_4 tetrahedron with decreasing P_2O_5 content in the glasses.[41),49] With increasing the Mg/P ratio in TiMg-IGs and NbMg-IGs, the integrated intensities of TiO_4 and NbO_4 increase, and those of TiO_6 and NbO_6 decrease. The titania and niobate in the glasses take the form of tetrahedra and cross-link the phosphate groups. The integrated peak intensities of $(PO_4)_{sym}$ (Q_p^0), POP_{sym} (Q_p^1), and P–O $(Q_p^1)_{term}$ showed good agreement with ^{31}P MAS-NMR results. However, it may seem that $(PO_3)_{sym}$ (Q_p^1) showed different behavior between TiMg-IGs and NbMg-IGs. In the ^{31}P MAS-NMR results, there was no significant difference in Q_p^0/Q_p^1 ratio between TiMg-IGs and NbMg-IGs. With increase in Q_p^0 content in the glass (i.e., increase in Mg/P ratio), the $(PO_4)_{sym}$ peak intensity increased. The weak $(PO_3)_{sym}$ band is close to the broad $(PO_4)_{sym}$ one. That is, the deconvolution accuracy of the $(PO_3)_{sym}$ band may be affected by the $(PO_4)_{sym}$ one, and the trend of $(PO_3)_{sym}$ peak intensity is difficult to be discussed here.

The ion dissolution rate increased with the Mg/P ratio; the chemical durability of the glasses decreased. Franks et al.[15] and Lee et al.[18] reported that the dissolution rate of MgO–CaO–Na_2O–P_2O_5 glasses within the metaphosphate region decreased with increasing the MgO content. Smith et al.[20] and Khor et al.[17] reported that the chemical durability of MgO–ZnO–P_2O_5 glasses in near the metaphospate region was improved by increasing the MgO content in the glasses. In our previous work, the chemical durability of CaO–P_2O_5–TiO_2 metaphosphate glasses improved with the addition of MgO, while that of the invert glasses decreased when CaO was substituted by MgO.[22),23] The chemical durabilities of TiMg-IGs and NbMg-IGs decreased with increasing the Mg/P ratio. This can possibly be explained by magnesium cross-linking the phosphate groups to form P–O–Mg bonds, similar to Si–O–Mg bonds, which weaken the glass network structure[50] and easily induce hydrolysis.[51] The dissolution rates of Ti^{4+} and Nb^{5+} ions on day 1 showed a similar trend to those of Mg^{2+} and P^{5+} ions. However, the dissolution rates of Ti^{4+} and Nb^{5+} ions after day 1 were smaller than those of Mg^{2+} and P^{5+} ions. The surfaces of the glasses were considered to be covered with gel-like oxide layers that contain titanium or niobium and phosphate. It may seem that the dissolution behavior of NbMg-IG with Mg/P = 1.00 has different trend between day 5 and 7 compared to those of the other glasses. From ^{31}P MAS-NMR and Raman spectra, the glass with Mg/P = 1.00 consists predominantly of Q_p^1 with a small amount of Q_p^0. This structure is almost similar to that of the other glass with the nearby composition, e.g., NbMg-IG with Mg/P = 1.10. The dissolution of NbMg-IGs is considered to be controlled between day 5 and 7, due to the formation of the gel-like oxide layers. Thus, a series of ion dissolution behavior of NbMg-IGs would be explainable, including that of the glass with Mg/P = 1.00.

5. Conclusions

The structures and dissolution behaviors of glasses containing TiO_2 or Nb_2O_5 with a large amount of MgO were investigated. Glasses with Mg/P ratios between 1.00 and 1.36 were successfully prepared by a conventional melt-quenching method. The intermediate oxides (TiO_2 or Nb_2O_5) and MgO in the glasses are proposed to act as network formers and create P–O–Ti/Nb and P–O–Mg bonds, respectively, which cross-link short phosphate chains (Q_p^0 and Q_p^1). Therefore, the glass-forming ability was

improved. The chemical durability of the glasses decreased with increasing the Mg/P ratio. Magnesium in the glasses entered the phosphate network to form P–O–Mg bonds, which weakened the glass network structure and induced hydrolysis. Mg^{2+} ions in this glass system were dissolved from the glasses relatively easily. These glasses may be candidates for Mg^{2+} ion-releasing biomaterials, which can accelerate cell adhesion, proliferation, and differentiation.

Acknowledgements This work was supported in part by JSPS KAKENHI Grant Numbers 25249094, 26289238, and 267992.

References

1) E. Kordes, W. Vogel and R. Feterowsky, *Z. Elektrochem.*, **57**, 282–289 (1953).
2) T. Okura, K. Yamashita and T. Kanazawa, *Phys. Chem. Glasses*, **29**, 13–17 (1988).
3) E. Matsubara, Y. Waseda, M. Ashizuka and E. Ishida, *J. Non-Cryst. Solids*, **103**, 117–124 (1988).
4) T. Kanazawa, *J. Non-Cryst. Solids*, **52**, 187–194 (1982).
5) G. Walter, R. Kranold, D. Stachel and W. Götz, *Phys. Chem. Glasses*, **31**, 188–195 (1990).
6) U. Hoppe, G. Walter and D. Stachel, *Phys. Chem. Glasses*, **33**, 216–221 (1992).
7) G. Walter, U. Hoppe, R. Kranold and D. Stachel, *Phys. Chem. Glasses*, **35**, 245–252 (1994).
8) U. Hoppe, G. Walter, R. Kranold, D. Stachel and A. Barz, *J. Non-Cryst. Solids*, **192–193**, 28–31 (1995).
9) K. Suzuya, D. L. Price, C. K. Loong and S. Kohara, *J. Phys. Chem. Solids*, **60**, 1457–1460 (1999).
10) F. Fayon, D. Massiot, K. Suzuya and D. L. Price, *J. Non-Cryst. Solids*, **283**, 88–94 (2001).
11) G. Walter, J. Vogel, U. Hoppe and P. Hartmann, *J. Non-Cryst. Solids*, **320**, 210–222 (2003).
12) M. A. Karakassides, A. Saranti and I. Koutselas, *J. Non-Cryst. Solids*, **347**, 69–79 (2004).
13) K. Meyer, *Phys. Chem. Glasses*, **42**, 79–87 (2001).
14) G. Walter, J. Vogel, U. Hoppe and P. Hartmann, *J. Non-Cryst. Solids*, **296**, 212–223 (2001).
15) K. Franks, V. Salih, J. C. Knowles and I. Olsen, *J. Mater. Sci.: Mater. Med.*, **13**, 549–556 (2002).
16) I. Ahmed, A. Parsons, A. Jones, G. Walker, C. Scotchford and C. Rudd, *J. Biomater. Appl.*, **24**, 555–575 (2010).
17) S. F. Khor, Z. A. Talib, W. M. Daud and H. A. A. Sidek, *J. Mater. Sci.*, **46**, 7895–7900 (2011).
18) I.-H. Lee, S.-H. Shin, F. Foroutan, N. J. Lakhkar, M.-S. Gong and J. C. Knowles, *J. Non-Cryst. Solids*, **363**, 57–63 (2013).
19) S. F. Khor, Z. A. Talib, F. Malek and E. M. Cheng, *Opt. Mater.*, **35**, 629–633 (2013).
20) C. E. Smith and R. K. Brow, *J. Non-Cryst. Solids*, **390**, 51–58 (2014).
21) R. Oueslati Omrani, A. Kaoutar, A. El Jazouli, S. Krimi, I. Khattech, M. Jemal, J.-J. Videau and M. Couzi, *J. Alloys Compd.*, **632**, 766–771 (2015).
22) S. Lee, A. Obata and T. Kasuga, *Bioceram. Dev. Appl.*, **1**, DOI:10.4303/bda/D110148 (2010).
23) H. Morikawa, S. Lee, T. Kasuga and D. S. Brauer, *J. Non-Cryst. Solids*, **380**, 53–59 (2013).
24) T. Okuma, *Nutrition*, **17**, 679–680 (2001).
25) M. Takeichi and T. S. Okada, *Exp. Cell Res.*, **74**, 51–60 (1972).
26) Y. Yamasaki, Y. Yoshida, M. Okazaki, A. Shimazu, T. Uchida, T. Kudo, Y. Akagawa, Y. Hamada, J. Takahashi and N. Matsuura, *J. Biomed. Res.*, **62**, 99–105 (2002).
27) F. I. Wolf and A. Cittadini, *Front. Biosci.*, **4**, d607–d617 (1999).
28) A. Saboori, M. Rabiee, F. Moztarzadeh, M. Sheikhi, M. Tahriri and M. Karimi, *Mater. Sci. Eng., C*, **29**, 335–340 (2009).
29) T. Kasuga and Y. Abe, *J. Non-Cryst. Solids*, **243**, 70–740 (1999).
30) A. Obata, Y. Takahashi, T. Miyajima, K. Ueda, T. Narushima and T. Kasuga, *ACS Appl. Mater. Interfaces*, **4**, 5684–5690 (2012).
31) I. Mazali, L. Barbosa and O. Alves, *J. Mater. Sci.*, **39**, 1987–1995 (2004).
32) T. Kasuga, Y. Hosoi, M. Nogami and M. Niinomi, *J. Am. Ceram. Soc.*, **84**, 450–452 (2001).
33) T. Kasuga, T. Hattori and M. Niinomi, *Phosphorus Res. Bull.*, **26**, 8–15 (2012).
34) H. Maeda, T. Miyajima, S. Lee, A. Obata, K. Ueda, T. Narushima and T. Kasuga, *J. Ceram. Soc. Japan*, **122**, 122–124 (2014).
35) T. Narushima, K. Ueda, T. Goto, H. Masumoto, T. Katsube, H. Kawamura, C. Ouchi and Y. Iguchi, *Mater. Trans.*, **46**, 2246–2252 (2005).
36) U. Kyosuke, T. Narushima, T. Goto, T. Katsube, H. Nakagawa, H. Kawamura and M. Taira, *Mater. Trans.*, **48**, 307–312 (2007).
37) M. Ouchetto, B. Elouadi and S. Parke, *Phys. Chem. Glasses*, **32**, 22–28 (1991).
38) R. K. Brow, D. R. Tallant, S. T. Myers and C. C. Phifer, *J. Non-Cryst. Solids*, **191**, 45–55 (1995).
39) S. Sakka, F. Miyaji and K. Fukumi, *J. Non-Cryst. Solids*, **112**, 64–68 (1989).
40) A. Flambard, J. J. Videau, L. Delevoye, T. Cardinal, C. Labrugère, C. A. Rivero, M. Couzi and L. Montagne, *J. Non-Cryst. Solids*, **354**, 3540–3547 (2008).
41) S. M. Hsu, J. J. Wu, S. W. Yung, T. S. Chin, T. Zhang, Y. M. Lee, C. M. Chu and J. Y. Ding, *J. Non-Cryst. Solids*, **358**, 14–19 (2012).
42) S. Lee, A. Obata and T. Kasuga, *J. Ceram. Soc. Japan*, **117**, 935–938 (2009).
43) A. Dietzel, *Ztschr. Elektrochem.*, **48**, 9–23 (1942).
44) R. K. Brow, D. R. Tallant, W. L. Warren, A. McIntyre and D. E. Day, *Phys. Chem. Glasses*, **38**, 300–306 (1997).
45) H. Segawa, N. Akagi, T. Yano and S. Shibata, *J. Ceram. Soc. Japan*, **118**, 278–282 (2010).
46) Y. Li, W. Weng, J. D. Santos and A. M. Lopes, *Phys. Chem. Glasses - Eur. J. Glass Sci. Technol. Part B*, **49**, 41–45 (2008).
47) A. El Jazouli, J. C. Viala, C. Parent, G. Le Flem and P. Hagenmuller, *J. Solid State Chem.*, **73**, 433–439 (1988).
48) F. F. Sene, J. R. Martinelli and L. Gomes, *J. Non-Cryst. Solids*, **348**, 30–37 (2004).
49) C. M. Chu, J. J. Wu, S. W. Yung, T. S. Chin, T. Zhang and F. B. Wu, *J. Non-Cryst. Solids*, **357**, 939–945 (2011).
50) S. J. Watts, R. G. Hill, M. D. O'Donnell and R. V. Law, *J. Non-Cryst. Solids*, **356**, 517–524 (2010).
51) D. S. Brauer, N. Karpukhina, G. Kedia, A. Bhat, R. V. Law, I. Radecka and R. G. Hill, *J. R. Soc., Interface*, **10**, 20120647 (2012).